Proceedings of the 11th World Congress on Electrical Engineering and Computer Systems and Sciences (EECSS'25)

Paris, France - August, 2025 Paper No. CIST 155 DOI: 10.11159/cist25.155

Optimal Multi-Objective Design of an Integrated INS/AHRS System in GPS-Denied Environments Using the Real-coded Memetic Algorithm

Davoud Darabi¹, Mohsen Fathi Jegarkandi ² and Hadi Nobahari³

^{1,2,3} Department of Aerospace Engineering, Sharif University of Technology Tehran, Iran davoud.darabi@ae.sharif.edu; fathi@sharif.edu; Nobahari@sharif.edu

Abstract - A novel meta-heuristic optimization algorithm is developed to solve multi-objective Multi-disciplinary Design Optimization (MDO) problems. The new algorithm, called multi-objective adaptive real-coded Memetic Algorithm (MARCOMA), is suitable for large scale optimization problems. MARCOMA is then applied to solve an MDO problem. The problem has many design variables and three disciplines including Navigation and guidance. Each discipline has its own design variables and analysis codes. Pitch Programming is used as the guidance law. A three-channel autopilot is used for stabilization during the separation phase and for executing guidance commands of the Aerial-Launched Vehicle (ALV) during flight phase. Navigation discipline has an inertial navigation system and attitude and heading reference system to estimate Euler angles at GPS-denied environment. For this purpose, Extended Kalman Filter parameters is optimized by measuring of angles to cooperate ALV to orbit. All disciplines are integrated in a 6-DOF flight simulation and the two objectives, elevation angle estimation and inverse of injection velocity, are minimized concurrently. The result is a Pareto set of non-dominated solutions within the performance space. The designer can choose an optimal solution based on his/her preferences and compromises. The examination of different initial condition scenarios shows the excellent performance of the optimization algorithm in solving the large-scale problem.

Keywords: GPS-Denied Navigation, Multi-Objective Optimization, Memetic Algorithm.

1. Introduction

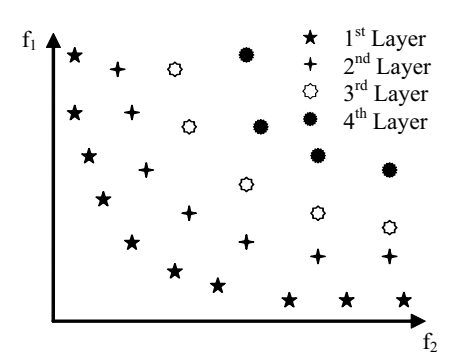
In real world applications, most of the design problems involve more than one engineering discipline. These problems are addressed as Multidisciplinary Design Optimization (MDO) problem. MDO has been widely used in design optimization of flying vehicles [1-5]. In the recent past, some authors employed gradient-based methods [6, 7]; however, modern approaches to MDO problems have been updated and are now more frequently utilized. Techniques such as evolutionary algorithms integrated with heuristic methods have emerged as dominant approaches. These methods benefit from high convergence rates and population diversity while requiring only the objective function and constraints eliminating the need for derivatives with respect to design variables. In contrast, gradient-based (GB) techniques often converge to local optima and struggle with nonlinear, multi-modal design problems. These limitations have spurred growing interest in direct, global heuristic optimization algorithms, including Memetic Algorithms (MAs), Evolutionary Algorithms (EAs), and other metaheuristics [2, 3, 5]. MDO problems have frequently more than one objective to be optimized. However, most of the researchers have solved single-objective MDO problems [1, 2, 4, 5]. Design of complex engineering systems often involves multiple interacting disciplines and conflicting objectives. In [3], MDO of some flying vehicles are studied using multiobjective (MO) optimization algorithms. Previous research works have employed simplification techniques like weighted sum aggregation or cost function transformation to solve multi-objective optimization problems. Such methodological simplifications inevitably propagate approximation errors into the optimization results, thereby leading to solutions that may substantially diverge from actual problem constraints and objectives [8, 9]. These remedies are useful for simple engineering designs, but the design outcomes are deteriorated for complicated systems such flying vehicles. Moreover, it cannot give the designer enough insight about the decision space of the design problem. The main idea to obtain the solution of a multiobjective optimization problem is the use of Pareto optimality condition [10].

There is an increasing interest in the application of EAs in multi-objective MDO problems [5]. The main reason to use EAs in MDO is the most similarity between the iterative design process toward an optimal design and the evolution process. Moreover, there are powerful meta-heuristics based on EAs and the field is rapidly growing up. EAs can also successfully cope with high-dimensional, multimodal, and noisy problems. The later comes from the fact that they don't require derivatives or gradients of the objective functions. They have also the capability of finding global optimum solutions amongst many local optima. Memetic Algorithms (MAs) are a class of modern meta-heuristics that combine EAs and Local Search (LS) techniques to find the global optimum. MAs apply a separate LS process to refine the new born individuals. An

important aspect concerning MAs is the trade-off between the exploration abilities of EAs and the exploitation abilities of the LS techniques. Previously, the authors developed an adaptive memetic algorithm for continuous problem domains (see references [12] for details). In this paper, first a new multi-objective adaptive real-coded memetic algorithm is described which is called Multi-objective Adaptive Real-Coded Memetic Algorithm (MARCOMA). The multi-objective MDO problem of an Aerial Launch Vehicle (ALV) has been solved using the MARCOMA. The problem involves five different disciplines including, navigation and guidance. The multi-objective algorithm optimizes concurrently 9 design variables in such a way that both inverse orbital injection velocity and standard deviation of pitch angle with respect to pitch programme of the ALV. The organization of the paper is as follows: in section 2, the new optimization algorithm, called MARCOMA is introduced. In section 3, MDO of a ALV is defined as a multi-objective optimization problem. Design constraints are introduced in section 4. Optimization results are presented in section 5. Finally, the conclusion is made in section 6.

2. Multi-objective Adaptive Real-coded Memetic Algorithm (MARCOMA)

Most MDO problems often have more than one objective function. Heuristic algorithms are very fit to cope with multiobjective problems. Among of the heuristic optimization algorithms, Memetic Algorithms are able to tackle with MO functions properly [13]. MARCOMA is the multi-objective variant of the recently developed MA, called Adaptive Realcoded Memetic Algorithm (ARCOMA) [12]. ARCOMA is composed of two main components: a real coded steady-state GA to provide exploration within the whole solution space, and a continuous LS scheme to exploit the most promising subspaces. ARCOMA utilizes continuous Ant Colony System (CACS) for LS. Since MARCOMA works with one more than one objective functions, Non-dominated Sorting (NS) strategy has solved this problem [12]. In this strategy, the population is categorized into a set of layers within the performance space. Each layer contains a set of non-dominated individuals. The first layer is called Pareto Frontier. The individuals of each layer dominate some individuals of the next layer. All of the nondominated individuals located in a layer have the same rank. Figure 1 shows the NS method for 2-dimension performance space. An individual which has better rank, will has more chance to select as a parent, on the basis of standard Replace Worst (RW) strategy. All of the individuals have same rank in a layer. In order to select a parent from a layer have used random selection. Crowding Distance Assignment (CDA) is utilized to procure monotone layer and discard an individual from crowded regions of population [12]. Figure 2 depicts the CDA method for 2-D performance space. Where, in Fig. 2, CDA is calculated for ith individual in all of the nth individuals. The operators of MARCOMA are similar to ARCOMA [12]. MARCOMA possess its own crossover, parent selector and replacement operators. More details will be described in the following.



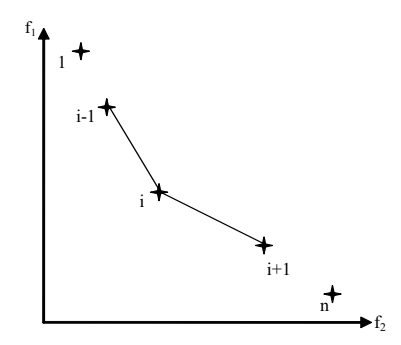


Fig. 1: Non-dominated Strategy for ranking of population Fig. 2: Crowded Distance Assignment in a layer of Pareto Frontier **2.1. Selection**

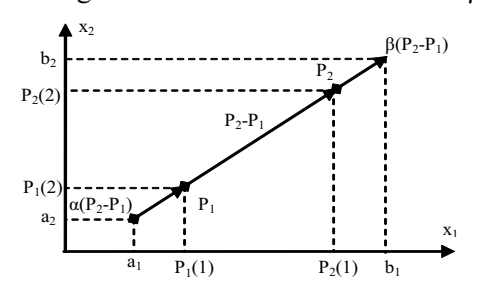
To generate each offspring, two parents must be selected from the mating pool. The new offspring is generated by using of crossover and mutation operators. The selection scheme adopted here is based on the Negative Assortative Mating (NAM) [14], as also proposed in [12]. In the NAM a first parent is selected by the roulette wheel method and NNAM chromosomes (NNAM = 3) are also selected with the same method. Then the similarity between each one of these chromosomes and the first parent is computed (similarity between two real-coded chromosomes is defined as the relative Euclidian distance). Then the one with less similarity is chosen to be the second parent.

2.2. Replacement

The standard Replace Worst (RW) is applied. In RW, offspring replaces the worst individual only if the new one is better. This strategy is adequate as a combination with LS, because it is an elitist strategy, and it is recommended for MAs. Furthermore, it offers a high selective pressure, making it a good complement for NAM [12].

2.3. Crossover

A new crossover method is developed in ARCOMA [12], which is based on BLX crossover method [15]. The new method carries out crossover within the direction of differences between two selected parents in the all-search space. The authors have considered two states for the parents. In the first state, suppose the case that in a specified dimension (1st dimension) first parent (P1) is smaller than second parent (P2). The authors introduce two parameters α and β that show the maximum allowed expansions along the subtraction vector P2-P1 to put the new offspring within the search interval (Figure 3). The following relations are derived for α i and β i: In this case, the "(1), (2)" are used (Fig. 3):



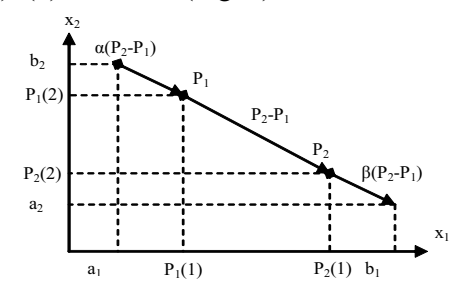


Fig. 3: Parent₂ (ith dimension) > Parent₁ (ith dimension)

Fig. 4: Parent₂ (ith dimension) < Parent₁ (ith dimension)

where i, is number of each dimension, ai and bi are lower and upper bound in ith dimension. In second state suppose that in a specified dimension (2nd dimension) the first parent (P₁) is bigger than that of the second parent (P₂). In this case the following relations (3), (4) are used (Fig. 4):

$$\alpha_{i} = \frac{P_{1}(i) - a(i)}{P_{1}(i) - P_{2}(i)}$$

$$\beta_{i} = \frac{b(i) - P_{2}(i)}{P_{1}(i) - P_{2}(i)}$$
(1)
$$\alpha_{i} = \frac{b(i) - P_{1}(i)}{P_{1}(i) - P_{2}(i)}$$
(2)
$$\beta_{i} = \frac{P_{2}(i) - a(i)}{P_{1}(i) - P_{2}(i)}$$
(4)

$$\beta_{i} = \frac{b(i) - P_{2}(i)}{P_{1}(i) - P_{2}(i)}$$

$$(2) \qquad \beta_{i} = \frac{P_{2}(i) - a(i)}{P_{1}(i) - P_{2}(i)}$$

Finally, with utilizing above equation for
$$\alpha_i$$
 and β_i , the crossover equation "(5)," is derived as follows:
$$P = P_1 - \alpha (P_2 - P_1) + (1 + \alpha + \beta) (P_2 - P_1) rand$$
 where α and β are the permissible values of α_i and β_i over all dimensions. (5)

2.4. Mutation

The Nun-uniform mutation has been used in this paper. If this operator is applied in generation k, and NPOP is the maximum number of generations then,

$$P_{i}^{'} = \begin{cases} P_{i} + \Delta \left(k, b_{i} - P_{i} \right) & \text{if } \tau = 0 \\ P_{i} - \Delta \left(k, P_{i} - a_{i} \right) & \text{if } \tau = 1 \end{cases}$$
 (6)

with τ being a random number which may have a value of zero or one, and

$$\Delta(t,y) = y\left(1 - rand\left(\frac{1 - k}{N_{Pop}}\right)^{b}\right) \tag{7}$$

where rand is a random number from the interval [0,1] and b is a parameter chosen by the user. In this research b=16. This function gives a value in the range (0, y) [12].

2.5. Local Search

MARCOMA utilizes a multi-objective variant of CACS entitled Multi-objective CACS (MOCACS). A simplified variant of CACS is utilized for LS. Like in CACS, to provide a continuous pheromone model over the search space, the pheromone distribution is considered in the form of a normal Probability Distribution Function (PDF) and ants choose their next destinations using a random generator with the PDF. The fitness is calculated in the new point and some knowledge about the search space is acquired, used to update the pheromone distribution. Basic distinction of MOCACS with respect to CACS is in sorting of individuals. MOCACS utilizes NS for ranking of the individuals. Here the history of the travelled points by the single ant is used to update pheromone. The number of search steps for LS (N_{il S}) and the ratio of local to global search domains (DR_{L2GS}) have been proposed by the authors as a new contribution. In other words, N_{iLS} and DR_{L2GS} are adapted based on the distribution of pheromone, when good solutions are closed to each other, pheromone distribution is

confined and vice versa. When pheromone distribution is confined, N_{iLS} is increased and DR_{L2GS} is decreased to permit the more concentrated LS and vice versa. N_{iLS} and DR_{L2GS} are calculated as follows:

where
$$x_i$$
 is the magnitude of each attribute in the ith dimension of and y_i is the corresponding fitness function. The * sign

$$I_{\rm ILS} = \left[N_{\rm LS} (x_i - x_i^*) / \sigma \right] \tag{9}$$

$$d_{\rm L2GS} = C_{\rm LS}\sigma \tag{10}$$

denotes the best solution found so far. Also, N_{LS} and C_{LS} are algorithm parameters that should be tuned and pheromone distribution. In MARCOMA, the global exploration is carried out in the whole search space and ants search within limited search intervals. MARCOMA is strongly proposed by the authors for large scale multi-objective problems like MDO. The population is initialized at the beginning of MARCOMA running. After that, all of the individuals are sorted by using of NS strategy. The population insert to main loop of MARCOMA and selection operator, choose Noffspring-th individuals to be parents. The crossover and mutation schemes are exerted on the parents. In this spot, LS process is applied on the offsprings and then replacement operator, tune the population. In the MARCOMA algorithm, to prevent premature convergence and getting trapped in local optima, the algorithm's convergence criterion is used. Specifically, the standard deviation of the objective function is divided by the mean of the objective functions, and if this fraction is less than the convergence threshold, the population is regenerated. The convergence threshold in this algorithm is 0.05, and the number of regenerated individuals in the population is 40% of the total population size. Flowchart of the MARCOMA can be seen in Figure 5. MARCOMA has six tuning parameters which have been tuned by the authors. Table 1 shows the tuned parameters.

Fig. 5: MARCOMA General Flowchart Table 1: MARCOMA Parameters

Parameters	Values	Descriptions
N _{POP}	20	Population size
$N_{offspring}$	2	Number of offspring's
N_{NAM}	3	Number of candidates as the second parent of NAM
N_{LS}	0.9	Local search iterations factor
C_{LS}	10	Local search interval factor
$P_{ m MUT}$	0.125	Mutation Probability

3. Definition of the MDO Problem

MDO of a ALV is defined in this section. The ALV is considered as Pegasus XL configuration [16]. Figure 6 shows a schematic of the Pegasus air-launch vehicle and the Lockheed L-1011 TriStar aircraft at the moment of initial stage separation and flight time history. Based on fig. 6, flight phases and stages separation are modelled and implemented at simulations scheme. Given the mandatory control system operation immediately after separation to ensure both (1) safe clearance from the carrier aircraft and (2) stability against aerodynamic disturbances generated by the aircraft's wake vortex, one of the critical challenges in air-launched satellite vehicles is navigation; where both the current and future attitude of the launch vehicle must be precisely determined. Launching from an aircraft introduces significant safety and navigational complexities. On one hand, the safety of the carrier aircraft must be ensured, while on the other, the launch vehicle requires accurate trajectory guidance.

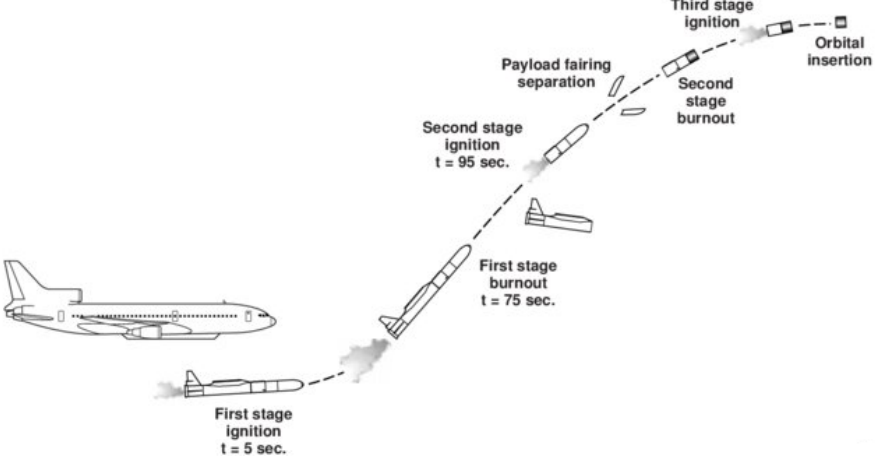


Fig. 6: Pegasus XL with L-1011 Aircraft

The primary navigation method for launch vehicles typically relies on an integrated INS/GPS system [17]. However, this paper addresses a key challenge: GPS denial due to magnetically disturbed environments and electromagnetic interference [18]. To overcome this limitation, the proposed solution assumes that the launch vehicle's Inertial Navigation System (INS) is augmented with an Attitude and Heading Reference System (AHRS). During low-acceleration phases (when the engine is off), the AHRS supplements the INS by providing pitch and roll angle corrections. Additionally, a separate magnetometer is employed for north-referenced heading estimation. To ensure high-accuracy attitude estimation, an extended Kalman filter (EKF) is implemented. The filter processes linear accelerations and angular velocities from the IMU (Inertial Measurement Unit) and integrates them with body-frame acceleration and gravitational acceleration measurements from the AHRS to estimate pitch and roll angles. A critical factor in achieving reliable estimation is the proper tuning of the process noise covariance matrix (Q) and the measurement noise covariance matrix (R). These matrices directly impact filter performance, and suboptimal values can lead to drift or instability. Therefore, in this study, the elements of Q and R are treated as design variables and are optimized to enhance navigation accuracy under GPS-denied conditions. A rigorous derivation of the EKF's state transition (process) and observation (measurement) equations can be found in [19]. To calculate the pitch angle using the AHRS sensor and Kalman filter under conditions where the launcher's acceleration is less than 1g, the Eq. 11 is used: In the 11.a equation, a_x is the AHRS-measured axial acceleration, and a_z is the AHRS-measured normal acceleration. Additionally, the roll angle is obtained from the Eq. 11.b:

$$\theta_m = \tan^{-1}\left(\frac{a_x}{a_z}\right); \varphi_m = \tan^{-1}\left(\frac{-a_z}{a_y}\right) - \frac{\pi}{2}$$
 (11.a,b)

The general equations of the Kalman filter are summarized below: The measurement vector includes three AHRS Euler angles as Eq. 12:

$$\mathbf{y}_{k} = \mathbf{H}_{k}\mathbf{x}_{k} + \mathbf{v}_{k} = \begin{bmatrix} \psi_{m} \\ \theta_{m} \\ \varphi_{m} \end{bmatrix} + \mathbf{v}_{k} \tag{12}$$

where: \mathbf{y}_k is measurement vector, \mathbf{H}_k is Observation matrix, $\mathbf{v}_k \sim \mathcal{N}(0, \mathbf{R}_k)$ is measurement noise and \mathbf{R}_k is Measurement noise covariance. Also process model (prediction) consists of state propagation and covariance prediction as Eq. 13 and 14 respectively:

$$\mathbf{x}_{k}^{-} = \mathbf{F}_{k-1} \mathbf{x}_{k-1}^{+} + \mathbf{B}_{k-1} \mathbf{u}_{k-1} + \mathbf{w}_{k-1}$$
(13)

$$P_k^- = F_{k-1} P_{k-1}^+ F_{k-1}^T + Q_{k-1} \tag{14}$$

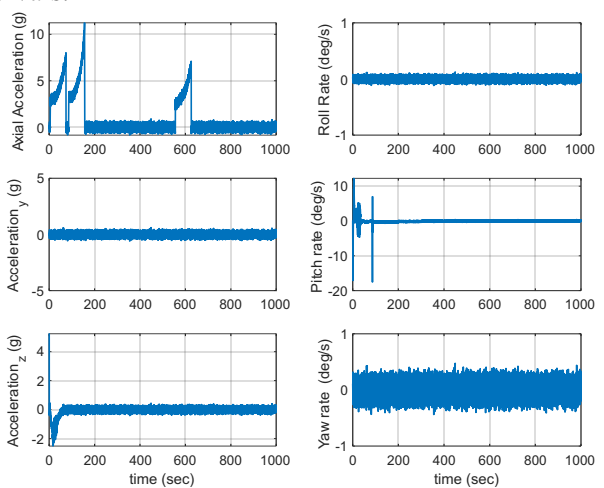
applicable), $w_{k-1} \sim \mathcal{N}(0, \mathbf{Q}_{k-1})$ is process noise, \mathbf{P}_{k}^{-} is predicted error covariance and \mathbf{Q}_{k-1} is process noise covariance. The

$$K_{k} = P_{k}^{-} H_{k}^{T} (H_{k} P_{k}^{-} H_{k}^{T} + R_{k})^{-1}; x_{k}^{+} = x_{k}^{-} + K_{k} (y_{k}^{-} H_{k} x_{k}^{-}); P_{k}^{+} = (I - K_{k} H_{k}) P_{k}^{-}$$
(15)

Kalman gain, state update and covariance update equations are Eq. 15 as follow: $K_k = P_k^- H_k^T (H_k P_k^- H_k^T + R_k)^{-1}; x_k^+ = x_k^- + K_k (y_k - H_k x_k^-); P_k^+ = (I - K_k H_k) P_k^-$ (15) The noise model used in this study for the rate-gyro and accelerometer IMU is based on the ADIS16488 sensor. Figure 7 shows the noise output of the accelerometers and gyros at simulation. The noise power used in simulations was set to: for accelerometers, Noise power (PSD) = $3 \times (0.00013)^2 = 5.437 \times 10^{-8}$ m²/s³, and for gyros, Noise power (PSD) = $3 \times (0.00013)^2 = 5.437 \times 10^{-8}$ m²/s³, and for gyros, Noise power (PSD) = $3 \times (0.00013)^2 = 5.437 \times 10^{-8}$ m²/s³, and for gyros, Noise power (PSD) = $3 \times (0.00013)^2 = 5.437 \times 10^{-8}$ m²/s³, and for gyros, Noise power (PSD) = $3 \times (0.00013)^2 = 5.437 \times 10^{-8}$ m²/s³, and for gyros, Noise power (PSD) = $3 \times (0.00013)^2 = 5.437 \times 10^{-8}$ m²/s³, and for gyros, Noise power (PSD) = $3 \times (0.00013)^2 = 5.437 \times 10^{-8}$ m²/s³, and for gyros, Noise power (PSD) = $3 \times (0.00013)^2 = 5.437 \times 10^{-8}$ m²/s³, and for gyros, Noise power (PSD) = $3 \times (0.00013)^2 = 5.437 \times 10^{-8}$ m²/s³, and for gyros, Noise power (PSD) = $3 \times (0.00013)^2 = 5.437 \times 10^{-8}$ m²/s³. $(0.00000063)^2 = 1.216 \times 10^{-12} \text{ rad}^2/\text{s}^3$. The problem involves two different disciplines for multi-objective multidisciplinary design, namely guidance and navigation. Utilizing the analysis codes of these disciplines, a 6-Degree of Freedom (6-DOF) flight simulation has been developed to solve the general equations of motion and to obtain the objective functions. The 6-DOF has aerodynamic, propulsion, autopilot and flight dynamics disciplines. Here, designer wants to simultaneously minimize both inverse orbital injection velocity and standard deviation of measured with respect to ideal pitch angle, which is obtained from solving the propagation equations in the simulation. The guidance discipline used pitch programmed scheme for pitch angle commands which was approximated using a piecewise exponential function that captures the essential characteristics of the desired attitude profile. The proposed pitch program approximation provides a smooth, parametric representation of the vehicle's attitude profile during ascent. The function captures the characteristic pitch-over maneuver through a continuous analytical formulation with physically interpretable parameters. The pitch angle $\theta(t)$ is modelled as a function of the independent variable t (typically time) using a composite exponential expression:

$$\theta(t) = \theta_f + (\theta_p - \theta_p) \cdot \left[1 - e^{-k_g t}\right] \cdot e^{-k_d (t - t_p)^{1.5}} \quad \text{for} \quad t \ge 0$$
(16)

where: θ_p = Peak pitch angle (design variable), θ_f = Final pitch angle (design variable), t_p = Peak time (design variable), k_g = Growth rate coefficient (design variable), k_d = Decay rate coefficient (design variable). The performance of the proposed pitch program approximation can be seen in Figure 8 by setting of: $\theta_p = 40^\circ$, $\theta_f = -28^\circ$, $t_p = 36$ s, kg = 0.15 s⁻¹, $k_d = 0.0005$ s⁻¹. This figure demonstrates that the optimized curve can be obtained by vertically adjusting the pitch angle values at fixed time intervals.



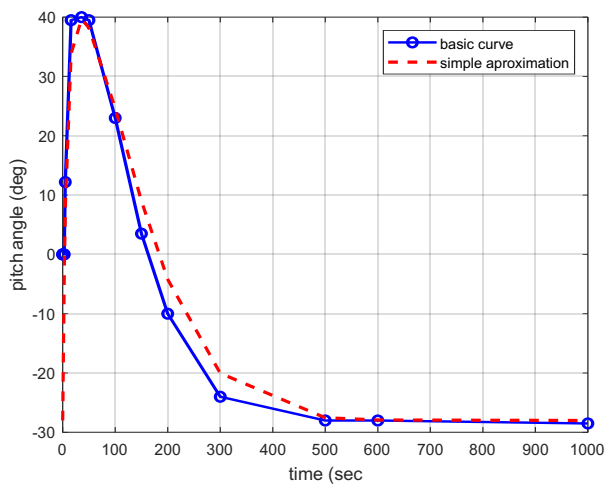


Fig. 7: the proposed pitch program approximation using piecewise exponential function

Fig. 8: the proposed pitch program approximation using piecewise exponential function

The Missile DATCOM software was employed to calculate aerodynamic force and moment coefficients for the 6-DOF simulation. The Pegasus launch vehicle configuration was modeled using this software, and the relevant coefficients were extracted. The NRLMSISE-00 atmospheric model was utilized for atmospheric simulation. The three-stage thrust profile of the aforementioned launch vehicle's engine was implemented in the simulation. Thrust Profile and mass time history of ALV depicted at figure 9 during flight simulation. A proportional controller with variable coefficients was designed for the roll channel. The PI controllers were implemented for both pitch and yaw channels. Aerodynamic fins and Thrust Vector Control (TVC) were employed for attitude control within the flight. All aerodynamic forces and moments, mass variations, center-of-mass changing, and inertia tensor were incorporated into the flight dynamics model. The equations of motion were solved with respect to the Earth-fixed inertial reference frame.

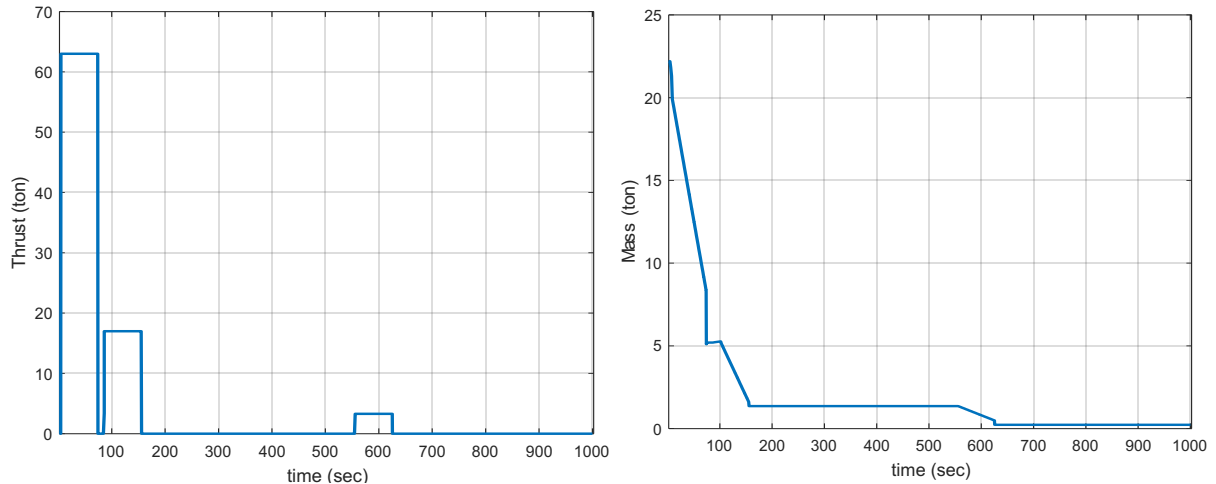


Fig.9: Approximate thrust profile (left) and mass versus time in flight time (right)

The optimization design variables of the above two disciplines have been listed in Table 2, including the corresponding search intervals. A total of 9 design variables across two disciplines were optimized. It should be noted that the yaw angle element in both the measurement and process noise matrices was held constant and was not included among the design variables.

TABLE 2 Design Variables and objective functions						
Disciplines	Design Variables	Min design space	Max design space	Descriptions		
	$\theta_{ m p}$	20 (deg)	80 (deg)	Peak pitch angle		
Guidance	$t_{\rm p}$	20 (sec)	40 (sec)	Peak time		
	$\theta_{ m f}$	-40 (deg)	0 (deg)	Final pitch angle		
	$k_{\rm g}$	0.001	1	Growth rate coefficient		
	k_d	0.001	1	Decay rate coefficient		
Navigation	Q(2,2)	10e-7	10e7	element of process noise matrix for θ (pitch angle)		
Navigation	Q(3,3)	10e-15	10e15	element of process noise matrix for θ (pitch angle)		
	R(2,2)	10e-7	10e7	element of measurement noise matrix for φ (roll angle)		
	R(3,3)	10e-15	10e15	element of measurement noise matrix for φ (roll angle)		
Objective fun	Objective functions Functions		Descriptions			
F ₁ =	$F_1 = 1/V_{bo}$		Inverse of orbital injection velocity			
$F_2 = std(\theta_i - \theta_{meas})$		standard deviation of measured with respect to ideal pitch angle				

4. Design Constraint Checking and Assumptions

After the MARCOMA optimization algorithm sends the design variables for evaluation to the objective function, two constraints are checked before running the six-degree-of-freedom simulation. This is done to prevent lengthy executions and unrealistic designs. One of these constraints is the error in the measured pitch angle compared to its true or ideal value. As mentioned earlier, the yaw angle is obtained using a magnetic north finder, which is not the subject of this research. Therefore, if the measured pitch and roll angles from the AHRS become singular, first constraint is applied such that a large penalty will be applied to the objective functions. The second constraint relates to the launcher's velocity at the desired altitudes for payload injection (altitudes greater than 500 km). It's important to explain that as the launcher's altitude increases during flight, the theoretical circular orbital velocity decreases. On the other hand, with increasing altitude and the ignition of the

launcher's third stage, the injection altitude reaches beyond 500 km. Therefore, in the times after the third stage ignites, the difference between the launcher's velocity and the circular orbital velocity is compared. If the launcher's velocity is greater than the orbital velocity, the cost function will be calculated; otherwise, a penalty will be applied to the cost function, and that design variable will automatically be removed from the memetic population. In any iterations of MARCOMA, all design attributes (an individual) insert to initialization of 6-DOF flight simulation code. After checking and meeting all mentioned assumptions and constraints, the guidance and navigation disciplines initializations run and it produces the command pitch angle and process and measurement noise covariance matrices (Q and R). Then, the system applies a 5g jettison impulse semi-parallel to gravity. Engine ignition occurs after a 5-second delay, during which aerodynamic stabilization is performed. Upon engine ignition, the Thrust Vector Control (TVC) system activates, executing pitch angle commands as determined by the optimization algorithm. The launch vehicle continues its powered ascent until reaching t+1000 seconds of flight time. Following termination of the six-degree-of-freedom (6-DOF) simulation, all objective functions are computed and finally passed to the optimization algorithm as the objective functions.

5. Results and Discussion

The Pareto frontiers obtained after evaluating 10000 design points are shown in Figure 10. In this figure 65 various pareto frontier are shown in lefts and final non-dominated solutions is depicted at right. The convergence of Pareto frontiers toward the origin of the two-dimensional performance space can be observed while the number of design evaluations proceeds. Each Pareto frontier contains the solutions that none of which can dominate any other (non-dominated solutions). The designer can select the final design point based on his/her compromises and/or preferences.

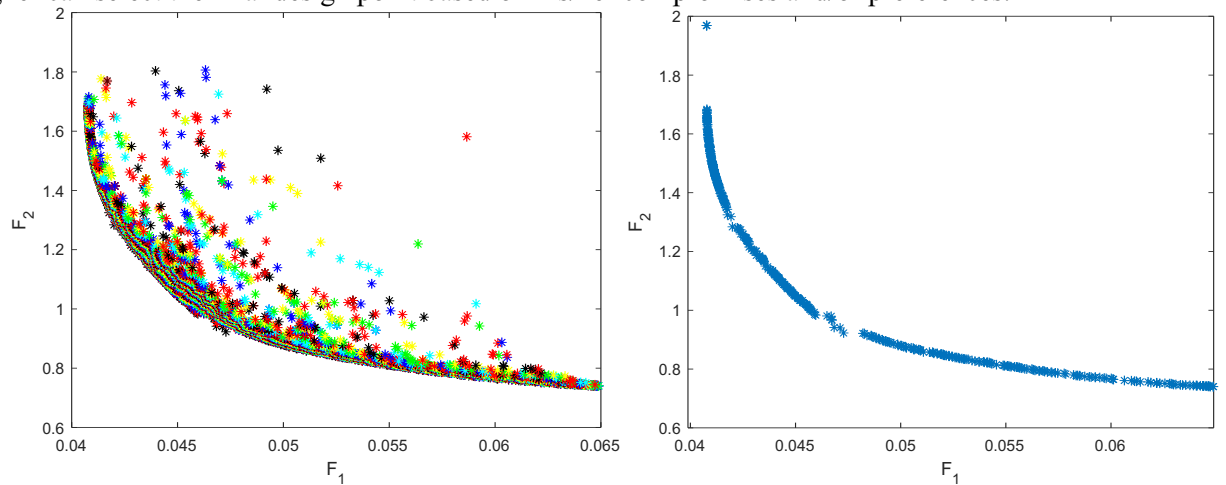


Fig. 10: 65 distinct pareto front at 10000 function evaluation (left)- final pareto front after 10000 function evaluation (right)

To demonstrate the trade-space analysis, a Pareto-optimal frontier point was selected using min-max normalization between competing objectives. The launch vehicle's simulated performance at this design point is shown below: "Figure 11 quantifies AHRS pitch angle accuracy under two conditions: (Left) Kalman-filtered estimation vs. truth-model simulation $(0.04^{\circ} \text{ std. dev.})$, and (Right) unfiltered AHRS vs. simulation $(0.07^{\circ} \text{ std. dev.})$. The filter reduces angular error by 40%, validating its efficacy for attitude determination.

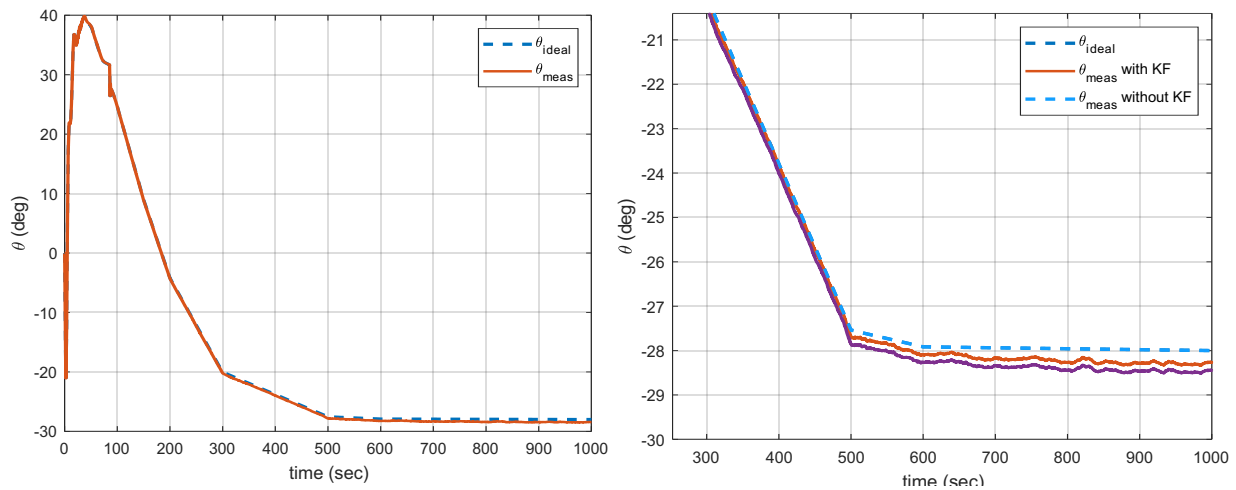


Fig.11: Kalman-filtered estimation vs. truth-model simulation (left)- unfiltered AHRS vs. simulation added (right)
Figure 12 characterizes the injection phase: (Left) Convergence of launch vehicle velocity with required orbital velocity
after t+600s, and (Right) Time-history of achieved orbital altitude, confirming successful payload insertion conditions.

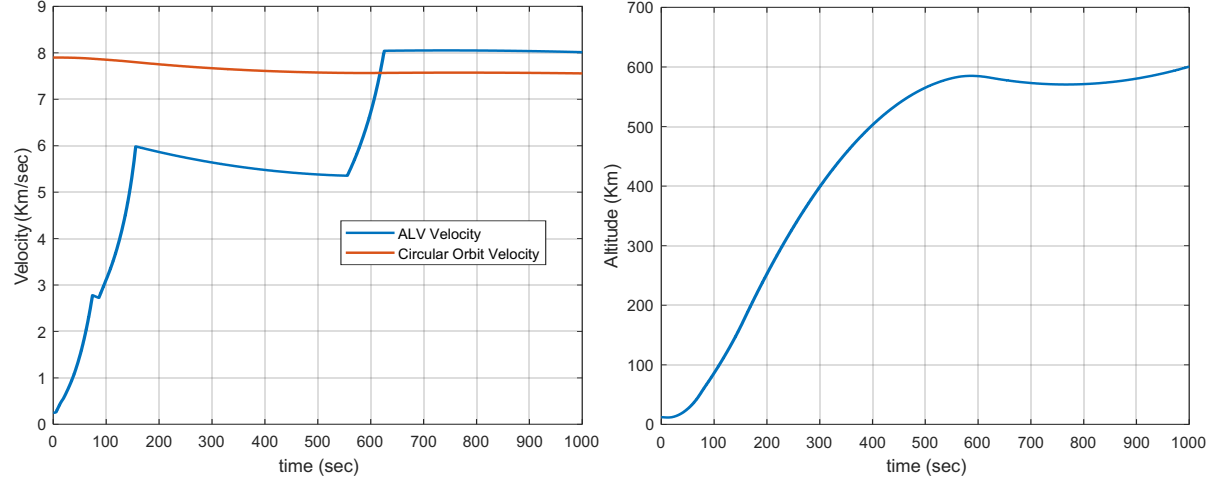


Fig.12: Convergence of launch vehicle velocity with required orbital velocity after t+600s (left)- Time-history of achieved orbital altitude (right)

6. Conclusion

This paper presents a novel multi-objective adaptive real-coded Memetic Algorithm (MARCOMA) designed to address complex Multidisciplinary Design Optimization (MDO) problems. Specifically, it focuses on the optimal multi-objective design of an integrated Inertial Navigation System (INS)/Attitude and Heading Reference System (AHRS) for an ALV operating in GPS-denied environments. The core problem tackled is the accurate estimation of Euler angles in environments where GPS signals are unavailable, integrating navigation, guidance, and control disciplines within a 6-Degree of Freedom flight simulation. To achieve high-accuracy attitude estimation, an Extended Kalman Filter (EKF) is implemented, and its critical parameters—the process noise covariance matrix (Q) and measurement noise covariance matrix (R)—are optimized as design variables. The guidance discipline employs a pitch programmed scheme, approximated by a piecewise exponential function, adding another set of design variables. The study concurrently minimizes two main objectives: the inverse orbital injection velocity and the standard deviation of the measured pitch angle relative to the ideal pitch angle. This multi-objective approach generates a Pareto set of non-dominated solutions, allowing designers to select an optimal solution based on their specific preferences and compromises. The optimization process involved a total of nine design variables across the guidance and navigation disciplines, with explicit design constraints checked before running the 6-DOF simulation to prevent unrealistic designs. MARCOMA demonstrates excellent performance in solving this large-scale MDO problem. It is a multiobjective variant of the Adaptive Real-coded Memetic Algorithm (ARCOMA), which combines a real-coded steady-state Genetic Algorithm (GA) for global exploration with a multi-objective adaptive variant of Continuous Ant Colony System

(CACS) for local exploitation. This hybrid approach effectively addresses the limitations of Evolutionary Algorithms (EAs), such as slower convergence rates, while maintaining their ability to find global optimum solutions in complex search spaces. Key features of MARCOMA include its Non-dominated Sorting (NS) strategy for ranking populations and Crowding Distance Assignment (CDA) to maintain population diversity.

The results obtained from evaluating 10,000 design points confirmed the effectiveness of the proposed system. Specifically, the Kalman-filtered AHRS pitch angle accuracy showed a significant reduction in angular error, achieving a 0.04° standard deviation compared to 0.07° for unfiltered AHRS, representing a 40% improvement. Furthermore, the optimization successfully ensured the launch vehicle's velocity converged with the required orbital velocity and reached the desired orbital altitude, confirming successful payload insertion conditions. In conclusion, this research successfully develops and applies MARCOMA for the optimal multi-objective design of an integrated INS/AHRS system for an Aerial Launch Vehicle, particularly in challenging GPS-denied environments. The methodology provides a robust and effective framework for addressing complex engineering design problems with conflicting objectives, offering significant advancements in autonomous navigation capabilities for aerospace applications.

References

- [1] N. F. Brown and J. R. Olds, "Evaluation of Multidisciplinary Optimization Techniques Applied to a Reusable Launch Vehicle," *Journal of Spacecraft and Rockets*, vol. 43, no. 6, pp. 1289–1300, Nov. 2006, doi: 10.2514/1.16577.
- [2] S. S. Chauhan, J. T. Hwang, and J. R. R. A. Martins, "An automated selection algorithm for nonlinear solvers in MDO," *Structural and Multidisciplinary Optimization*, vol. 58, no. 2, 349–377, Aug. 2018, doi: 10.1007/s00158-018-2004-5.
- [3] S. H. Pourtakdoust and A. H. Khodabakhsh, "Reliability-based multidisciplinary design optimization of an aeroelastic unpowered guided aerial vehicle," *Proceedings of the Institution of Mechanical Engineers, Part G: Journal of Aerospace Engineering*, vol. 237, no. 15, pp. 3463–3485, Dec. 2023, doi: 10.1177/09544100231198160.
- [4] A. Benaouali and A. Boutemedjet, "Multidisciplinary analysis and structural optimization for the aeroelastic sizing of a UAV wing using open-source code integration," *Aircraft Engineering and Aerospace Technology*, vol. 96, no. 4, pp. 585–592, May 2024, doi: 10.1108/AEAT-11-2023-0310.
- [5] J. Karimi, M. R. Rajabi, S. H. Sadati, and S. M. Hosseini, "Multidisciplinary design optimization of a dual-spin guided vehicle," *Defence Technology*, vol. 37, pp. 133–148, Jul. 2024, doi: 10.1016/j.dt.2023.11.025.
- [6] Vanderplaats Research & Development, Inc., DOT: Design Optimization Tools, Version 4.20, Goleta, CA, 1995.
- [7] Dulikravich, G. S., López, F., Koldakov, R. D., & Harchev, S. G. Multidisciplinary analysis and design optimization. In *Mini-Symposium on Inverse Problems, Brazilian Congress on Applied and Computational Mathematics*, Belo Horizonte, Brazil, September 10–13, 2001.
- [8] Cristina Bazgan, Stefan Ruzika, Clemens Thielen, Daniel Vanderpooten, "The Power of the Weighted Sum Scalarization for Approximating Multiobjective Optimization Problems," *Theory of Computing Systems*, vol. 66, pp. 395–415, 2022, doi: 10.1007/s00224-021-10066-5.
- [9] G. Zhu, M. Ye, X. Yu, J. Liu, M. Wang, Z. Luo, H. Liang, and Y. Zhong, "Optimizing Route Planning via the Weighted Sum Method and Multi-Criteria Decision-Making," *Mathematics*, vol. 13, no. 11, p. 1704, 2025, doi: 10.3390/math13111704.
- [10] Pareto, Manual of Political Economy, Augustus M. Kelley, New York, 1971.
- [11] A. M. Oliveira and C. S. Cerqueira, "A systematic review of MDO methods applied to launch vehicle design and their contributions to concurrent engineering," *Discover Mechanical Engineering*, vol. 4, no. 1, p. 19, 2025, doi: 10.1007/s44245-025-00104-8.
- [12] H. Nobahari and D. Darabi, "A New Adaptive Real-coded Memetic Algorithm," *International Conference on Artificial Intelligence and Computational Intelligence (AICI2009)*, Shanghai, China, 2009.
- [13] M. Lapucci, P. Mansueto, and F. Schoen, "A memetic procedure for global multi-objective optimization," *Mathematical Programming Computation*, vol. 15, no. 2, pp. 227–267, 2023.
- [14] C. Fernandes and A. C. Rosa, "Self-adjusting the intensity of assortative mating in genetic algorithms," *Soft Computing*, vol. 12, pp. 955–979, 2008, doi: 10.1007/s00500-007-0265-9.
- [15] A. Cervantes-Castillo, E. Mezura-Montes, and C. A. C. Coello, "An empirical comparison of two crossover operators in real-coded genetic algorithms for constrained numerical optimization problems," 2014 IEEE International Autumn

- Meeting on Power, Electronics and Computing (ROPEC), Ixtapa, Mexico, 2014, pp. 1–5, doi: 10.1109/ROPEC.2014.7036347.
- [16] Northrop Grumman Corporation, Pegasus Payload User's Guide, Release 8.2, 2020.
- [17] C. Jiang, S. B. Zhang, and Q. Z. Zhang, "A new adaptive h-infinity filtering algorithm for the GPS/INS integrated navigation," *Sensors*, vol. 16, no. 12, p. 2127, 2016, doi: 10.3390/s16122127.
- [18] Y. Chang, Y. Cheng, U. Manzoor, and J. Murray, "A review of UAV autonomous navigation in GPS-denied environments," *Robotics and Autonomous Systems*, vol. 170, p. 104533, 2023, doi: 10.1016/j.robot.2023.104533.
- [19] Gebre-Egziabher, Demoz, Roger C. Hayward, and J. David Powell. "Design of multi-sensor attitude determination systems." *IEEE Transactions on aerospace and electronic systems*, no. 2, 2004: 627-649.